Preparation of aniline from photocatalytic reduction of nitrobenzene using Pt/ Nd_2O_3 nanocomposite

R.M. Mohamed

PII: S0925-8388(15)30365-0
DOI: 10.1016/j.jallcom.2015.06.217
Reference: JALCOM 34625

To appear in: *Journal of Alloys and Compounds*

Received Date: 8 May 2015
Revised Date: 19 June 2015
Accepted Date: 28 June 2015

Please cite this article as: R.M. Mohamed, Preparation of aniline from photocatalytic reduction of nitrobenzene using Pt/ Nd_2O_3 nanocomposite, *Journal of Alloys and Compounds* (2015), doi: 10.1016/j.jallcom.2015.06.217.

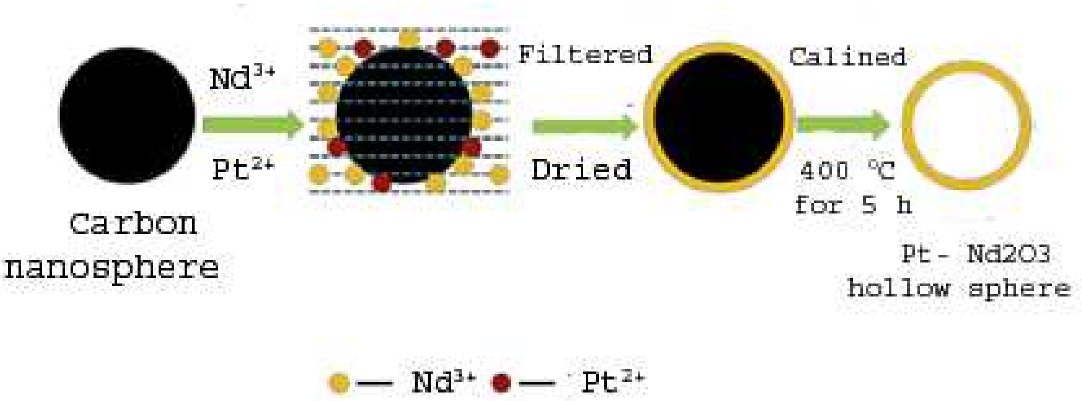
Carbon nanosphere
Nd^{3+}
Pt^{2+}
Filtered
Dried
Calined
400 °C
for 5 h
Pt - Nd2O3
hollow sphere
● — Nd^{3+} ● — Pt^{2+}

Preparation of aniline from photocatalytic reduction of nitrobenzene using Pt/ Nd_2O_3 nanocomposite

R. M. Mohamed,[1] *

[1]Chemistry Department, Faculty of Science, King Abdulaziz University, P.O. Box 80203 Jeddah 21589, Saudi Arabia,

*Corresponding author, E-mail: mhmdouf@gmail.com; Tel.: +966-540715648; Fax: +966-2-6952292

Abstract

In this manuscript, a template method was used to synthesis Pt-doped Nd_2O_3 nanostructures with controlled Pt doping contents. The characterizations illustrated that the obtained samples have ultra high surface area (190 m^2/g), high crystallinity , small grain size (20 nm) and hollow spherical like morphology. Also, the band gap of the Pt-doped Nd_2O_3 nanostructures can be controlled by controlling the Pt contents. The photocatalytic activity of the Pt-doped Nd_2O_3 nanostructures samples was studied by studying the reduction of nitrobenzene into aniline using visible light irradiation. The photocatalytic performance of Nd_2O_3 was enhanced by Pt doping. This can be attributed to the fact that the trapping effect of the Pt-doped Nd_2O_3 nanostructures and the red shift of absorption edge. The study result provides an effective method to create different photocatalysts with enhanced visible-light-driven photocatalytic performance.

Keywords: Nd_2O_3; Pt Doping ; Visible absorption; Aniline synthesis

1.Introduction

The intermediates keys in the preparation of agrochemicals, pharmaceuticals and dyes are aromatic amines[1]. One of the most common method which used for preparation of amines is a hydrogenation method. The drawback for the hydrogenation method is poor efficiency and toxicity of metal used for hydrogenation [2]. Thus, from economic and environmental point of view, an effective method for cheap and cleaner fabrication of amine is remain a challenge in synthesis of organic. Recently, the photoreduction method is an effective and clean method for preparation of amine for organic synthesis[3]. TiO_2 is one of the most promising photocatalyst due to thermal and chemical stability, nontoxicity as well as its low cost. P_{25} Degussa has high photocatalytic activity due to separation between electron and hole between rutile (20%) and anatase (80 %)[4]. The first example of photoreduction of nitroaromatic compounds to aniline under UV irradiation using P_{25} Degussa is reported by Li et al [5]. Many researchers were tried to convert absorption of TiO_2 from UV to visible region or design new materials absorb in visible region. The first examples of photoreduction of nitro compounds using dye-sensitized TiO_2–P_{25} [6] or $PbBiO_2X$,[7] under LED irradiation were reported by Konig and co-workers. Ag–TiO_2, TiO_2 (anatase) and TiO_2–P_{25}, and under solar and UV-A light irradiation were used for preparation of ketones from ketoximes by Swaminathan and co-workers[8]. TiO_2–P_{25}, Pt–TiO_2, and Ag–TiO_2 nanoparticles under UV and solar light were used for preparation of indazole and benzimidazoles[9]. Single-crystalline rutile TiO_2 nanorods was used for preparation of benzaldehyde from photocatalytic oxidation of benzyl alcohol under visible light[10]. Synthesis of aldehydes and ketones from the corresponding oximes using sunlight irradiation were reported by activated amorphous TiO_2 incorporated into periodic mesoporous organosilicas [11]. From the green chemistry point view, still need to develop methods for preparing organic compounds using solar energy[12]. Therefore, the aim of this work is preparation of a new visible photocatalyst for synthesis of aniline from reduction of nitrobenzene.

2. Experimental

2.1. Materials synthesis

The hydrothermal method which was reported by Li et al [13] was used to prepare carbon spheres. To prepare the Pt-doped Nd_2O_3 nanostructures, 1 mmol of Neodymium(III) nitrate hexahydrate and stoichiometric amount of Platinum (II) chloride were dissolved in100 mL of N,N-dimethylformamide. 50 mg of as-synthesized carbon spheres was added to above mixture and the resulting mixture was sonicated for 40 min, then the resulting mixture was stirred for 24 h at room temperature. The resulting mixture was filtered many times by distilled water and ethanol. The obtained Pt-doped Nd_2O_3 nanostructures was dried at 80 ˚C for 24 h, then calcined at 400 ˚C in air for 5 h. The changeable concentrations of Pt in Pt-doped Nd_2O_3 nanostructures could be attempted by controlling the ratio of Neodymium(III) nitrate hexahydrate and Platinum (II) chloride (1:0, 1:0.01, 1:0.02, 1:0.03, 1:0.04, 1:0.05) in the solution. The contents of Pt in Nd_2O_3 were 0, 1, 2, 3, 4 and 5 % by molar ratio. The corresponding products were marked as 1N, 2 N, 3 N, 4 N, 5 N and 6 N, respectively.

2.2. Photocatalyst characterization

A Bruker Axis D8 using Cu Kα radiation (λ = 1.540 Å) was used to determine the X-ray diffraction patterns of the Nd_2O_3 and Pt-doped Nd_2O_3 nanostructures. A Nova 2000 series Chromatech apparatus was used to measure the BET surface area of the Nd_2O_3 and Pt-doped Nd_2O_3 nanostructures. Before measurement, the samples were heated under vacuum for 3 h at 200 °C. A UV/Vis/NIR spectrophotometer (V-570, JASCO, Japan) was used to measure the band gap energy of the Nd_2O_3 and Pt-doped Nd_2O_3 nanostructures. A JEOL-JEM-1230 microscope was used to determine the shape and particle size of the Nd_2O_3 and Pt-doped Nd_2O_3 nanostructures. Before measurement, the samples were dispersed in ethanol for 30 min. Then, a small portion of the samples were placed on a carbon-coated copper grid. A Thermo Scientific K-ALPHA, X-ray photoelectron spectroscope (XPS), England, was used to determine the elemental nature of the sample. The photoluminescence emission spectra of Before measurement, were measured using a Shimadzu RF-5301 fluorescence spectrophotometer.

2.3. Photocatalytic activity

Photocatalytic device consists of two parts was used to study photocatalytic application The first part is an annular quartz tube. For visible light source, Xenon lamp(500 W)covered by UV cut-off filter was used. It laid in annular tube and it temperature kept at about 30 °C by cooling by water. The second part is laid below the Xenon lamp and it consist of sealed quartz reactor with a diameter of 8.3 cm and The distance between the light source and the surface of the reaction solution is 11 cm. Before each photocatalytic reaction, definite weight of photocatalyst sample was dispersed ultrasonically into 10 ml of mixture of nitrobenzene-methanol(1:99, volume per volume). 8.13×10^{-4} mol/l is initial concentration of nitrobenzene. Before start of irradiation, to remove dissolved oxygen from reaction medium, N_2 gas was passed through reaction medium for 30 min. During reaction time, samples were taken for analysis using gas chromatography Agilent GC 7890A model: G3440A Gas Chromatography using 19091J-413 capillary column (30 m× 0.32 µm×0.25 µm) and chromatographic conditions applied for photocatalytic reduction of nitrobenzene are summarized in Table 1

3. Results and discussions

3.1. Characterization of photocatalyst

3.1.1. X-ray diffraction study

X-ray diffraction (XRD) was used for characterization the crystallographic structure of the products. Fig.1. shows XRD patterns of the Nd_2O_3 and Pt-doped Nd_2O_3 nanostructures. The results demonstrated that XRD pattern of Nd_2O_3 was in readily agreement with XRD pattern of Nd_2O_3 phase (PDF#74- 2139). Also, with increasing Pt contents, there is no peaks of platinum oxide or other phases could be detected in the Pt-doped Nd_2O_3 nanostructures samples, suggesting that the doping of platinum does not effect on the crystallization properties of Nd_2O_3. Because, the platinum concentrations were a little low and the radius of Pt^{2+} (94 pm) is smaller than that of Nd^{3+} (112 pm) and, so Pt^{2+} may be doped into the crystal lattice of Nd_2O_3 as shown in XRD patterns as shifting of main peak. of Nd_2O_3 at 2- theta = 30.8 which inset of Fig.1 to high value , forming a platinum- neodymium oxide finite solid solution.

3.1.2. SEM and TEM examination

Fig.2. shows SEM images of Nd_2O_3 with different Pt contents. The results reveal that addition of Pt does not change the morphology of the Nd_2O_3. The shape of all samples is spherical with diameter ranging from 100 to 200 nm. Also, we noticed that the shell of the spheres was composed of nanoparticles with small size. Fig.3. shows TEM image for 5 N sample. The result demonstrates that the thickness of the shell was about 8 nm and large numbers of pores were existed in the shell.

3.1.3. XPS analysis

Fig.4. shows the XPS spectra of 5 N sample in Pt 4f. The results reveal that platinum present as Pt $^{2+}$ ion due to the present of Pt 4 f 7/2 peak as 72.4 eV, which confirm the doping of Pt $^{2+}$ ion into the crystal lattice of Nd_2O_3 as shown before in XRD patterns as shifting of main peak.

3.1.4. BET surface areas and pore distributions

Fig.5. shows nitrogen adsorption–desorption isotherms of 5 N sample. The results reveal that the category of nitrogen adsorption–desorption isotherms of Pt- doped Nd_2O_3 nanostructure is type IV with distinct hysteresis loops observed in the relative pressure range of 0.6–0.90. It was clearly indicated that the products were mesoporous materials, which agreed well with the morphologies and microstructures of porous Nd_2O_3 products (Fig. 3). Also, the other samples have similar isotherm and pore diameter. BET surface area of as- prepared samples are listed in Table 2. The results demonstrated that the value of BET surface areas of Pt- doped Nd_2O_3 nanostructure is higher than that of Nd_2O_3 due to the introduce of Pt $^{2+}$ ion into lattice of Nd_2O_3.

3.1.5. Optical properties measurements

Fig.6. shows the UV–Vis spectra of Nd_2O_3 and Pt- doped Nd_2O_3 nanostructures. The results reveal that the red shift of absorption edge from 362 to 466 nm was occurred by doing of Pt into crystal lattice of Nd_2O_3 . The band gap of Nd_2O_3 and Pt- doped Nd_2O_3 nanostructures was calculated from their UV-Vis spectra and was tabulated in Table 3. The values of band gap are 3.42, 3.15, 2.98, 2.87, 2.73 and 2.66 eV, for 1 N, 2 N,3 N , 4 N , 5 N and 6 N samples, respectively, which means the band gap was decreased from 3.42 to 2.66 , eV by increased wt % of Pt doped into Nd_2O_3 nanostructures from 0 to 5 wt %, respectively.

Pl spectra of Nd_2O_3 and Pt- doped Nd_2O_3 nanostructures is shown in Fig.7. The results reveal that Pl intensity was decreased as wt % of Pt doped Nd_2O_3 nanostructures increased. This means Pt can capture electron from a conduction band of Nd_2O_3. Therefore, this leads to an increase in the life time required for e-h pair recombination and an increase of photocatalytic activity, as shown in photocatalytic activity part.

3.2. Photocatalytic reduction of nitrobenzene

3.2.1. Effect of the type of photocatalyst

Fig.8. shows effect of type of photocatalyst on photocatalytic reduction of nitrobenzene. Nitrosobenzene and aniline are the main compounds, which are detected by gas chromatography (GC). There is no detection by GC for aniline or nitrosobenzene in the absence of light or catalyst. The results reveal that the photocatalytic activity of 1 N and 2 N is very small (about 5 %) due Nd_2O_3 and 1 wt % Pt doped Nd_2O_3 absorb in UV region and photocatalytic was carried out under visible region. Also, increase wt % of Pt from 2 to 4 % increase photocatalytic activity from 53 to 98 %, respectively. Above 4 wt % of Pt has no significant effect on photocatalytic activity. Therefore, 4 wt % of Pt is an optimum condition for doping at which photocatalytic reduction of nitrobenzene reach to 98 % after 60 min reaction time. The reaction kinetics and rate constants for the effect of type of photocatalyst on reduction of nitrobenzene were studied and calculated as shown in Fig.9. and Table 4. The results show that the order of reaction is first order with respect to [nitrobenzene].

3.2.2. Effect of the amount of the photocatalyst

The effect of the loading of 4 wt % Pt doped Nd_2O_3 photocatalyst on photocatalytic reduction of nitrobenzene is shown in Fig. 10. The results reveal that the photocatalytic activity increased from 83 to 100 % after 60 min by increasing the weight of 4 wt % Pt doped Nd_2O_3 photocatalyst from 0.3 to 0.6 g/l. The reaction time decreased from 60 to 40 min by increasing the weight of 4 wt % Pt doped Nd_2O_3 photocatalyst from 0.6 to 0.9 g/l due to the increase in available active sites for the photocatalytic reaction. Additionally, we noticed that the photocatalytic activity decreased by increasing weight of 4 wt % Pt doped Nd_2O_3 photocatalyst above 0.9 g/l because the high weight of the photocatalyst will hinder the penetration of light during the reaction and decrease the available active sites for the photocatalytic reaction, decreasing the overall photocatalytic activity. The reaction kinetics and rate constants for the effect of amount of photocatalyst on reduction of nitrobenzene were studied and calculated as shown in Fig.11. and Table 5. The results show that the order of reaction is first order with respect to [nitrobenzene].

3.2.3. Recycling the photocatalyst

Testing the photocatalyst multiple times is an important factor for the commercial use of the photocatalyst. Fig. 10 shows the activity of 4 wt % Pt doped Nd_2O_3 photocatalyst that was recycled five times. The results demonstrate that the photocatalytic activity remained unchanged after being recycled five times. The results demonstrate that 4 wt % Pt doped Nd_2O_3 photocatalyst was stable after being recycled five times. Therefore, the 4 wt % Pt doped Nd_2O_3 photocatalyst can be recycled and separated easily.

3.3. Mechanisms

Noble metal-semiconductor nanocomposites, such as Pd-TiO_2 [14], Ag-TiO_2 [15], can be highly active photocatalysts due to synergy between the basis material and the surface plasmon resonance effect of noble metals. A similar effect was considered responsible for the photocatalytic reduction of nitrobenzene on Pt/Nd_2O_3. Visible-light irradiation excited Pt/Nd_2O_3 due to the surface plasmon resonance of Pt nanoparticles and electron-hole pairs on the surface of Pt nanoparticles. Nd_2O_3 excellent electron mobility could increase Pt/Nd_2O_3 charge transport rate, inhibit charge recombination and promote photocatalytic activity. GC results showed that the main products were nitrosobenzene and aniline. The mechanisms of photocatalytic reduction of NB over are as follows:

(1) Light generates hole-electron pairs. When photons with energy equal to or larger than the band gap irradiate Pt/Nd_2O_3, electrons transfer from the valence band to conduction band, producing oxidative photogenerated valence holes (h^+) and reductive conduction electrons (e^-) (Eq. 1).

(2) Photogenerated holes and electrons without recombination move to photocatalyst's surface.

(3) Photogenerated carriers react with adsorbents. CH_3OH solvent captures the holes, producing HCHO oxide and reductive $H^\cdot$ (Eqs. 2 and 3). Photogenerated electrons and $H^\cdot$ reduce NB, producing more nitrosobenzene and aniline (Eq. 4).

$$Pt/Nd_2O_3 + \text{Visible light} \longrightarrow Pt/Nd_2O_3\ (e^- + h^+) \qquad (1)$$

$$CH_3OH + h^+ \longrightarrow CH_3O^{\bullet} + {}^{\bullet}CH_2OH \qquad (2)$$

$$CH_3O^{\bullet} + {}^{\bullet}CH_2OH \longrightarrow 2H^{\bullet} + 2HCHO \qquad (3)$$

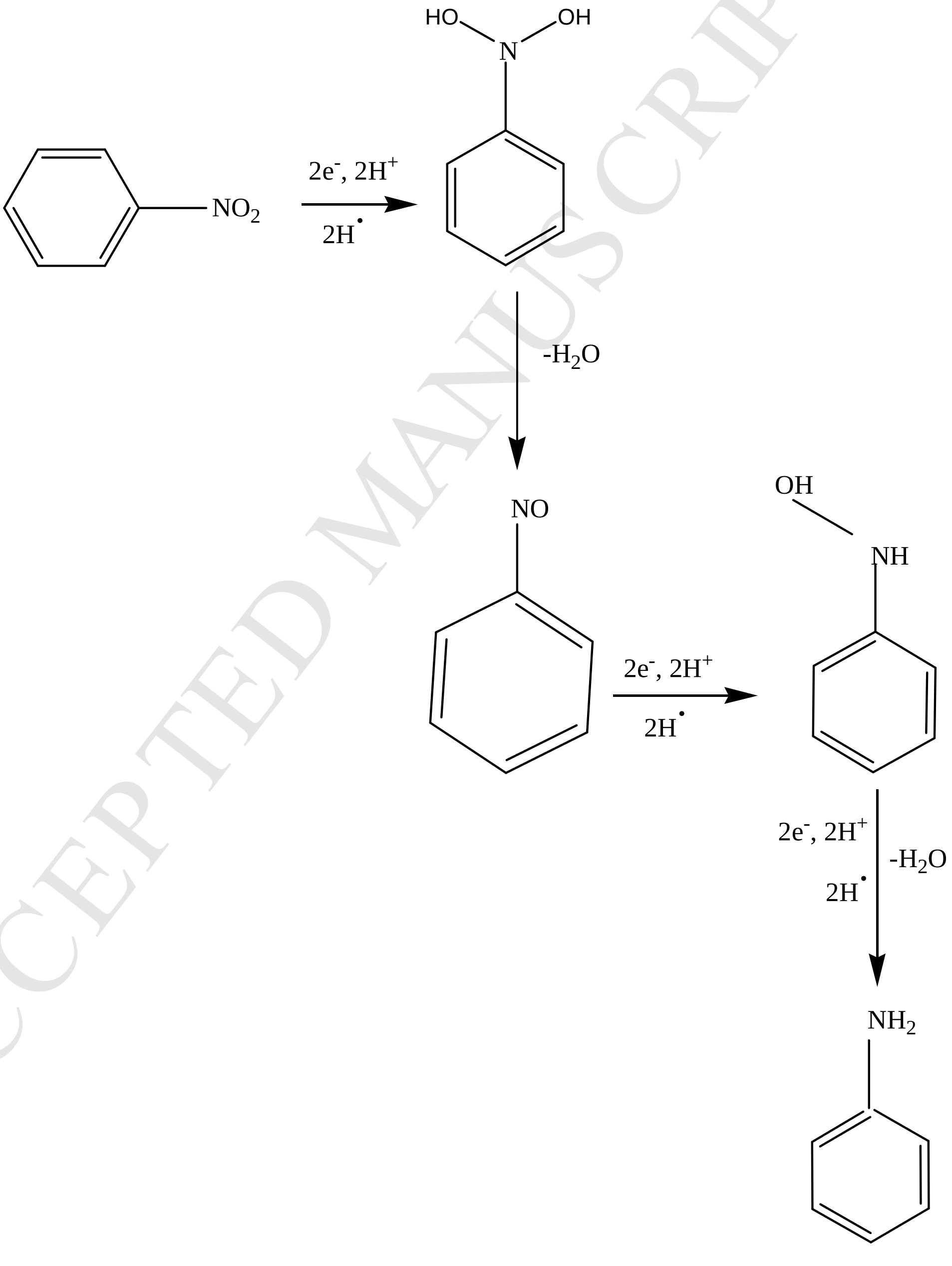

(4)

4. Conclusion

We have prepared the Pt doped Nd_2O_3 nanostructures with controlled Pt doping contents using a template method . The band gap of the Pt doped Nd_2O_3 could be tuned by controlling Fe doping contents. We found that increasing of Pt doping content, increasing the shift of absorption edge to visible region. Also, the separation and transformation of the photo-excited electrons and holes could be enhanced with appropriate Pt^{2+} ions doping contents. Therefore, the 4 wt % Pt doped Nd_2O_3 nanostructures have the highest photocatalytic efficiency under visible light. We can synthesize different photocatalysts with enhanced visible-light-driven photocatalytic performance using a template method.

Acknowledgement

This work was funded by the Deanship of Scientific Research (DSR), King Abdulaziz University, Jeddah, under grant number (130-521-D1435). The authors, therefore, acknowledge with thanks DSR technical and financial support.

References

[1] S.J. Kumar, M.M. Ho, T. Toyokuni, Tetrahedron Lett. 42(2001) 5601- 5603.

[2] K. Yanada, H. Yamaguchi, H. Meguri, S. Uchida, J. Chem. Soc., Chem. Commun. (1986) 1655-1656.

[3] G. Kuzmanich, A. Natarajan, K.K. Chin, M. Veerman, J.C. Mortko, A.M. Garcia-Garibay, J. Am. Chem. Soc., 130(2008) 1140-1141.

[4] S. Bakardjieva, J. Subrt, V. Stengl, J.M. Dianez, M. Sayagues, J. Appl. Catal. B, 58 (2005) 193-202.

[5] Y. Li, H. Wang, E.R. Partch, J. Org. Chem. 62 (1997) 5222-5225.

[6] S.Fuldner, T. Mitkina, T. Trottmann, A. Frimberger, M. Gruber, B. Konig, Photochem. Photobiol. Sci. 10 (2011) 623-625.

[7] S. Fuldner, P. Pohla, H. Bartling, S. Dankesreiter, R. Stadler, M. Gruber, A. Pfitzner, B. Konig, Green Chem. 13 (2011) 64-643.

[8] K. Selvam, B. Krishnakumar, R. Velmurugan, M. Swaminathan, Catal. Commun. 11 (2009) 280-284.

[9] K. Selvam, M. Swaminathan, Tetrahedron Lett., 52(2011) 3386-3392.

[10] J.G. Li, R.G. Xu, B. Zhang, R.J. Gong, Appl. Catal. B, 115–116(2012) 201-208.

[11] S. Abedi, B. Karimi, F. Kazemi, M. Bostina, H. Vali, Org. Biomol. Chem. 11 (2013) 416- 419.

[12] J. Baxter, X.Z. Bian, G. Chen, D. Danielson, S.M. Dresselhaus, G.A. Fedorov, S.T. Fishe, W.C. Jones, E. Maginn, U. Kortshagen, A. Manthiram, A. Nozik, R.D. Rolison, T. Sands , L. Shi, D. Sholl, Y.Y. Wu, Environ. Sci. 2(2009) 559-588.

[13] X. Sun, Y. Li, Angew. Chem. Int. Ed. 43 (2004) 597–601.

[14] M.Y. Abdelaal, R.M. Mohamed, J. Alloys Compd. 576 (2013) 201-207.

[15] R.M.Mohamed, I.A. Mkhalid, J. Alloys Compd. 501 (2010)301-306.

Figures Caption

Fig. 1. XRD patterns of the as-prepared samples.

Fig.2. SEM images of the as-prepared samples.

Fig.3. TEM image of 5 N sample.

Fig.4. XPS spectra of 5 N sample in Pt 4f.

Fig.5. nitrogen adsorption–desorption isotherms and corresponding pore diameter distribution curve(insets) of 5 N sample.

Fig.6. UV-Vis spectra of Nd_2O_3 and Pt- doped Nd_2O_3 nanostructures.

Fig.7. Pl spectra of Nd_2O_3 and Pt- doped Nd_2O_3 nanostructures.

Fig. 8. Effect of type of photocatalyst on the photocatalytic reduction of nitrobenzene.

Fig.9. Rate constant of reaction kinetic for photocatalytic reduction of nitrobenzene by different photocatalyst

Fig.10.Effect of amount of 4 wt % Pt doped Nd_2O_3 photocatalyst on the photocatalytic reduction of nitrobenzene.

Fig.11. Rate constant of reaction kinetic for effect of catalyst amount on reduction of nitrobenzene

Fig. 12. Recycling and reuse of 4 wt % Pt doped Nd_2O_3 photocatalysts for the photocatalytic reduction of nitrobenzene.

Table 1: Chromatographic conditions applied for photocatalytic reduction of nitrobenzene.

Item	Reduction of nitrobenzene
Oven	50°C for 5 min →200 °C 50→ 200 °C 10 °C/min
Detector	Type: FID Heater: 300 °C H2 flow: 30 ml/min Air flow: 400 ml/min Makeup flow: 25 ml/min
Injection	Heater: 250 °C Pressure:13.762 psi Total flow: 41.384 ml/min Septum purge flow: 3 ml/min Mode: split with ratio (10:1)
Column	(30 m× 0.32 µm×0.25 µm)

Table 2. Texture parameters of Nd_2O_3 and Pt- doped Nd_2O_3 nanostructure.

Sample	S_{BET} (m^2/g)	S_t (m^2/g)	S_{micro} (cm^2/g)	S_{ext} (cm^2/g)	V_p (cm^3/g)	r (Å)
1 N	190 .00	192.00	105.00	85.00	0.200	40.00
2 N	205.00	206.00	110.00	95.00	0.210	35.00
3 N	211.00	212.00	112.00	98.00	0.225	32.00
4 N	215.00	217.00	115.00	100.00	0.235	28.00
5 N	220.00	223.00	118.00	102.00	0.240	24.00
6 N	225.00	226.00	120.00	105.00	0.244	22.00

Table 3 : Band gap energy of Nd_2O_3 and Pt- doped Nd_2O_3 nanostructure.

Sample	Band gap energy, eV
1 N	3.42
2 N	3.15
3 N	2.98
4 N	2.87
5 N	2.73
6 N	2.66

Table 3: Rate constant of reaction kinetic for photocatalytic reduction of nitrobenzene by different photocatalyst

Sample	k x 10^{-5}, min^{-1}.
1 N	365
2 N	448
3 N	5237
4 N	13208
5 N	13498
6 N	14613

Table 4 : Rate constant of reaction kinetic for effect of catalyst amount on reduction of nitrobenzene

Sample	k x 10^{-5}, min^{-1}.
0.3 g/l	13208
0.6 g/l	13498
0.9 g/l	20316
1.2 g/l	18517
1.5 g/l	1281

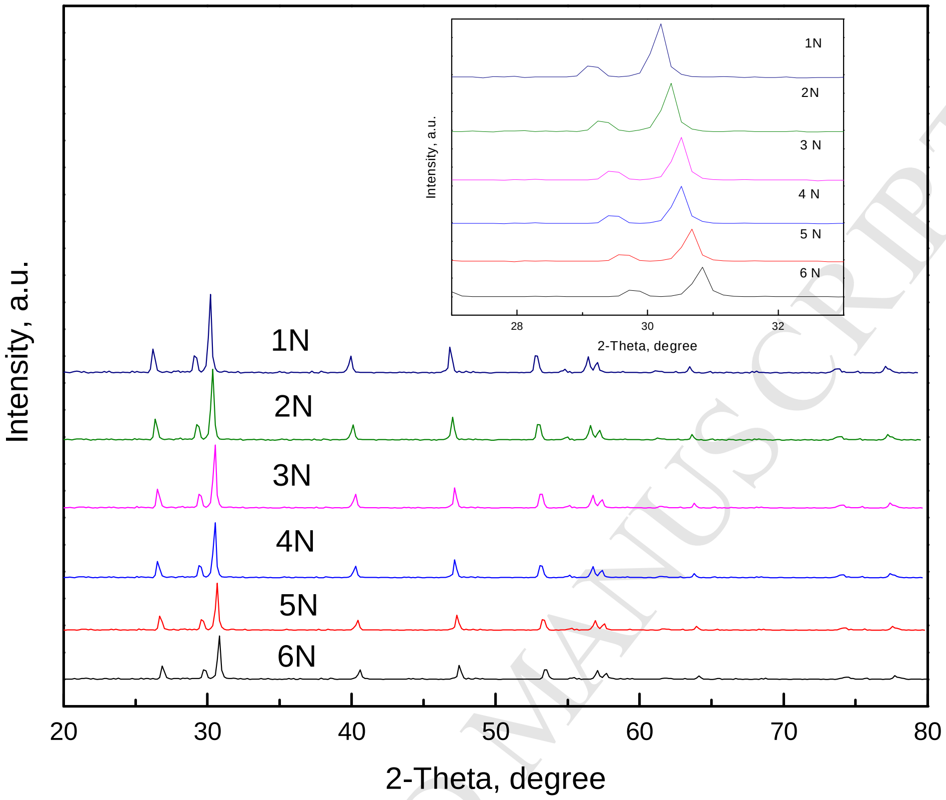
Intensity, a.u.
1N
2N
3N
4N
5N
6N
20
30
40
50
60
70
80
2-Theta, degree
Intensity, a.u.
1N
2N
3 N
4 N
5 N
6 N
28
30
32
2-Theta, degree

Fig.1.

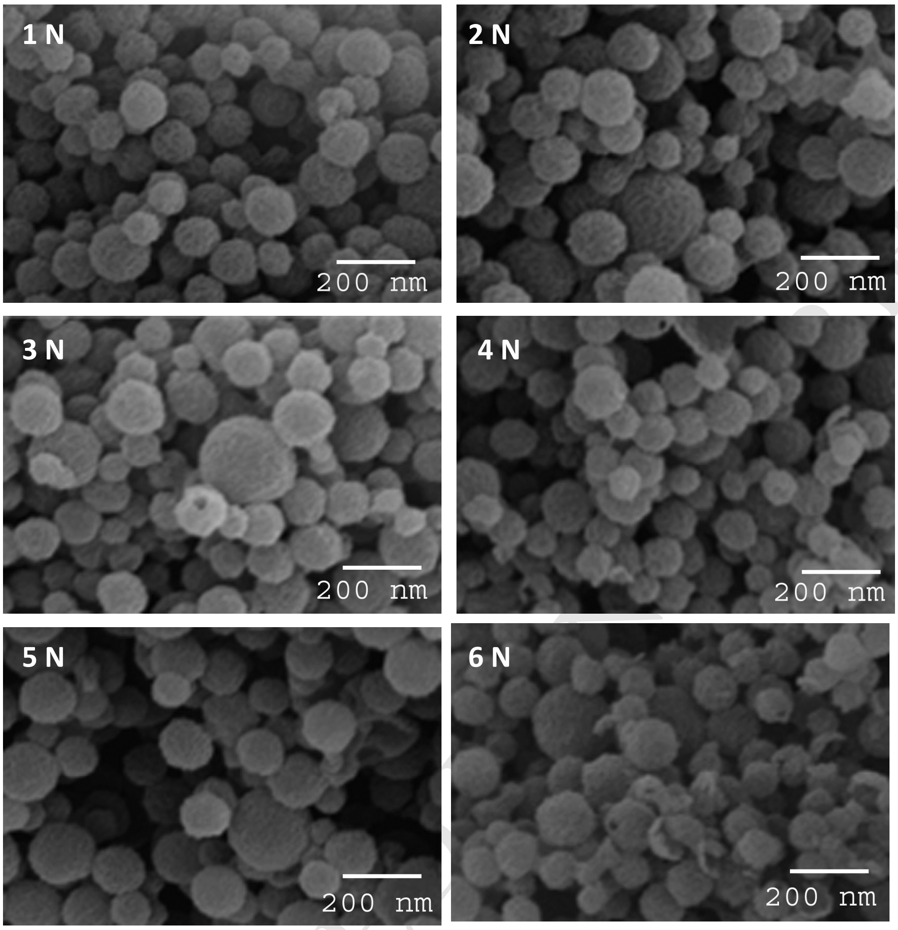

Fig.2.

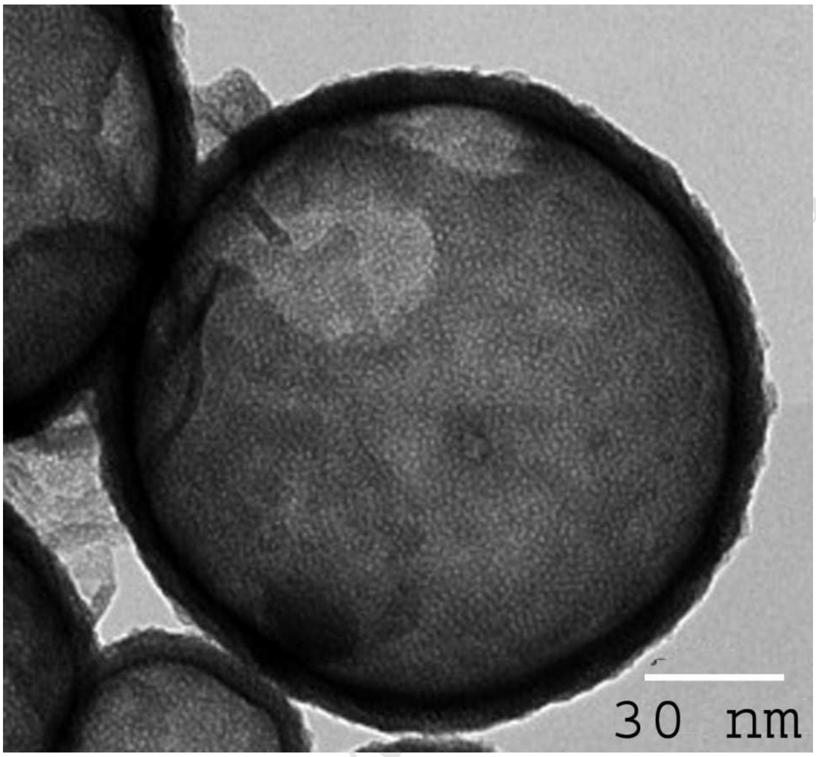

Fig.3.

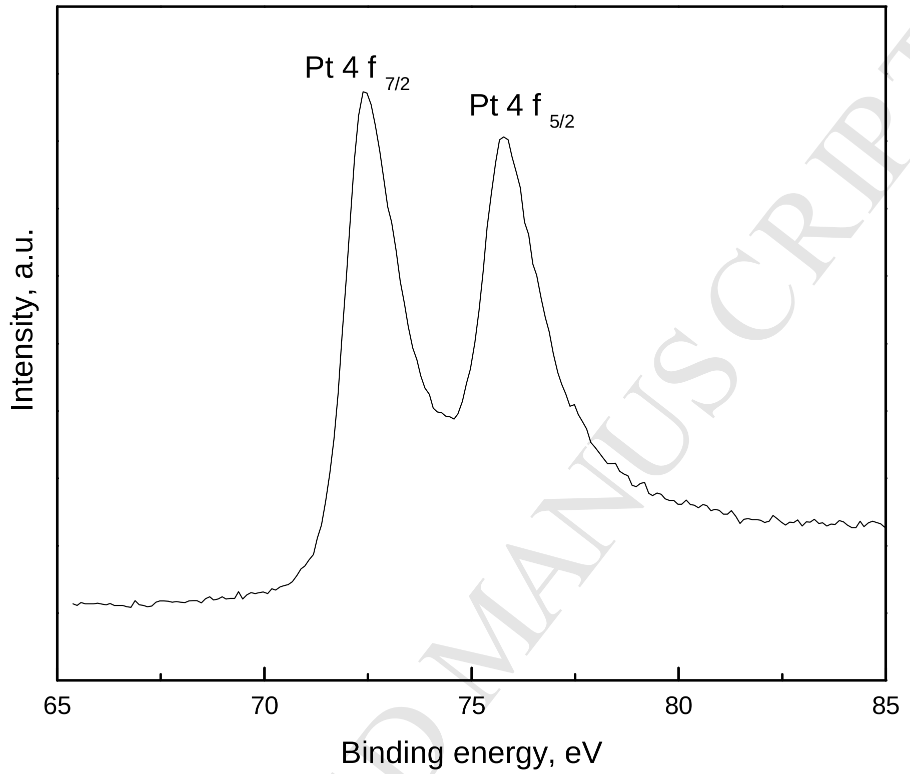

Fig.4.

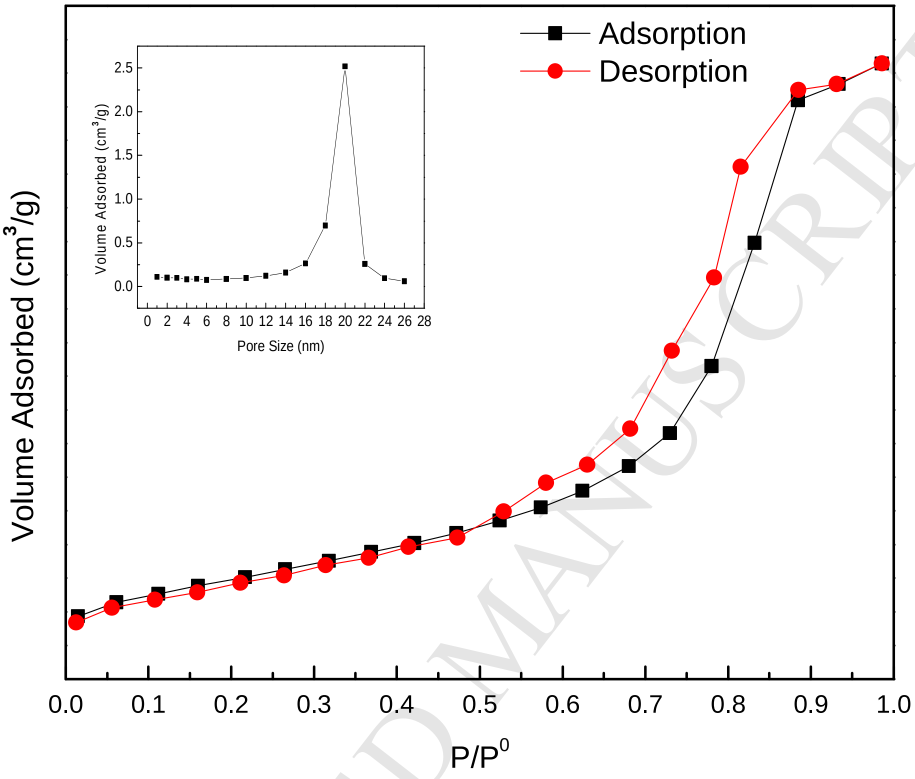
Adsorption
Desorption
Volume Adsorbed (cm3/g)
P/P0
0.0
0.1
0.2
0.3
0.4
0.5
0.6
0.7
0.8
0.9
1.0
Volume Adsorbed (cm3/g)
Pore Size (nm)
0.0
0.5
1.0
1.5
2.0
2.5
0
2
4
6
8
10
12
14
16
18
20
22
24
26
28

Fig.5.

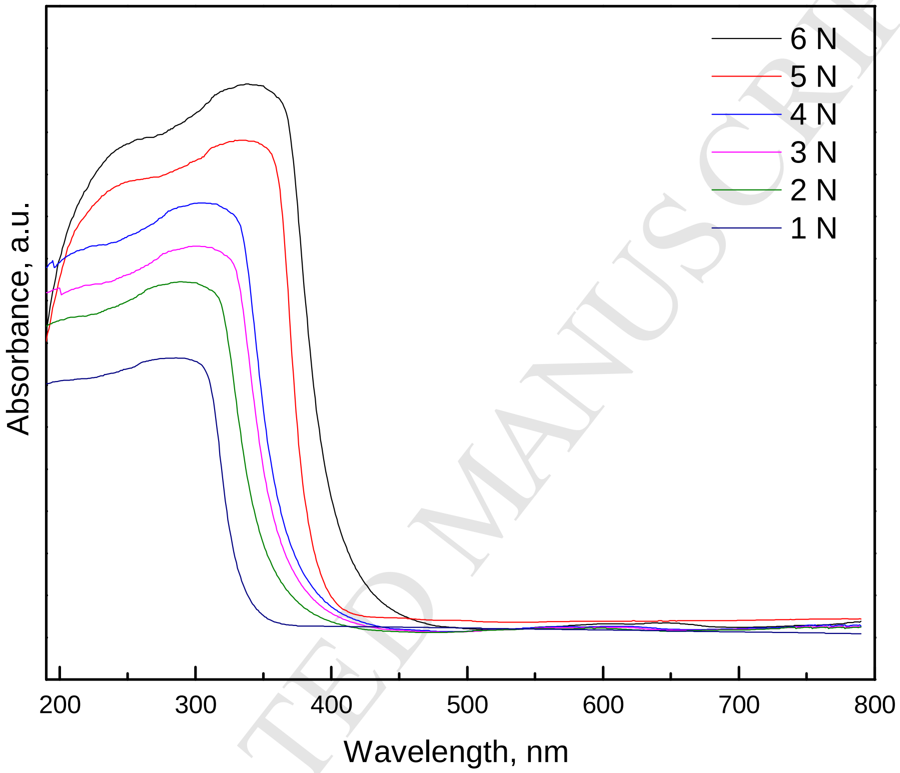
6 N
5 N
4 N
3 N
2 N
1 N
Absorbance, a.u.
200
300
400
500
600
700
800
Wavelength, nm

Fig.6.

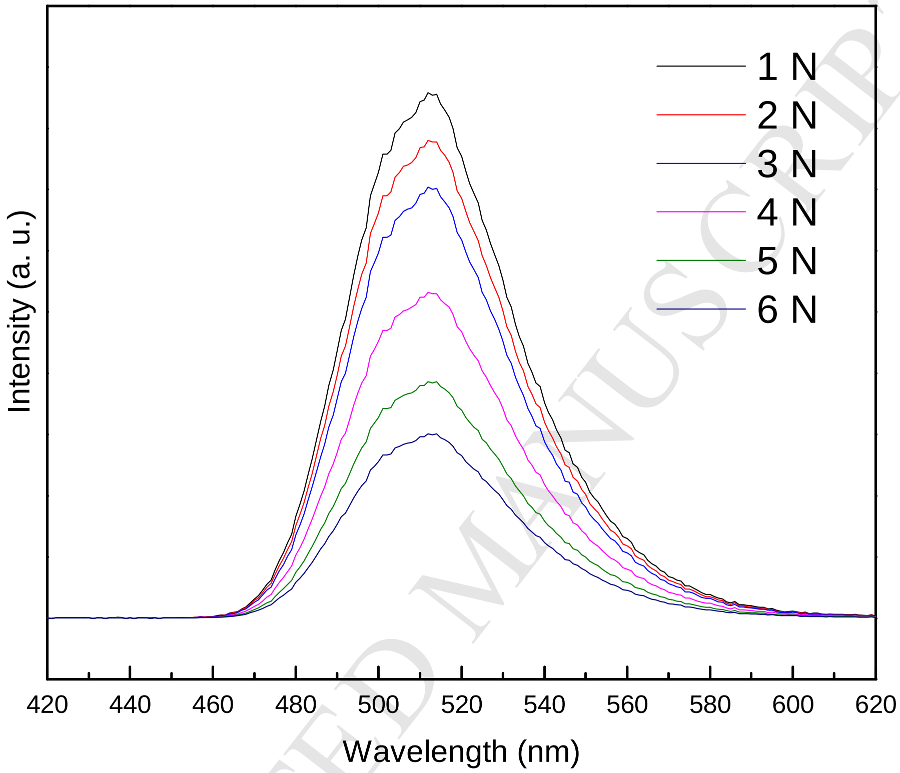
1 N
2 N
3 N
4 N
5 N
6 N
Intensity (a. u.)
420
440
460
480
500
520
540
560
580
600
620
Wavelength (nm)

Fig.7.

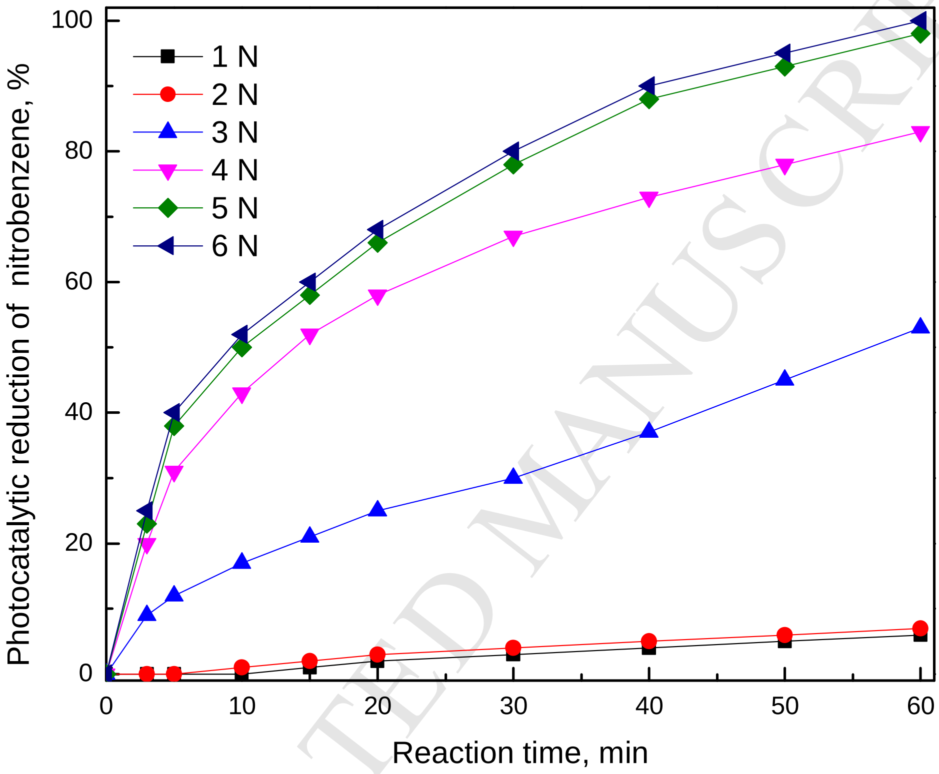
Photocatalytic reduction of nitrobenzene, %
Reaction time, min
0
20
40
60
80
100
0
10
20
30
40
50
60
1 N
2 N
3 N
4 N
5 N
6 N

Fig.8.

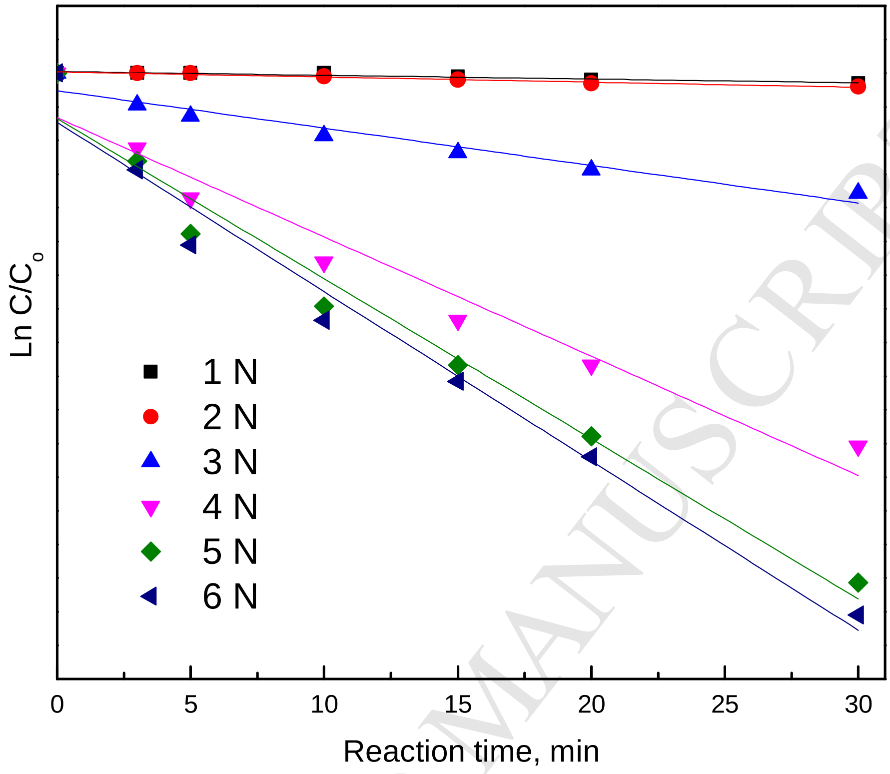

Fig.9.

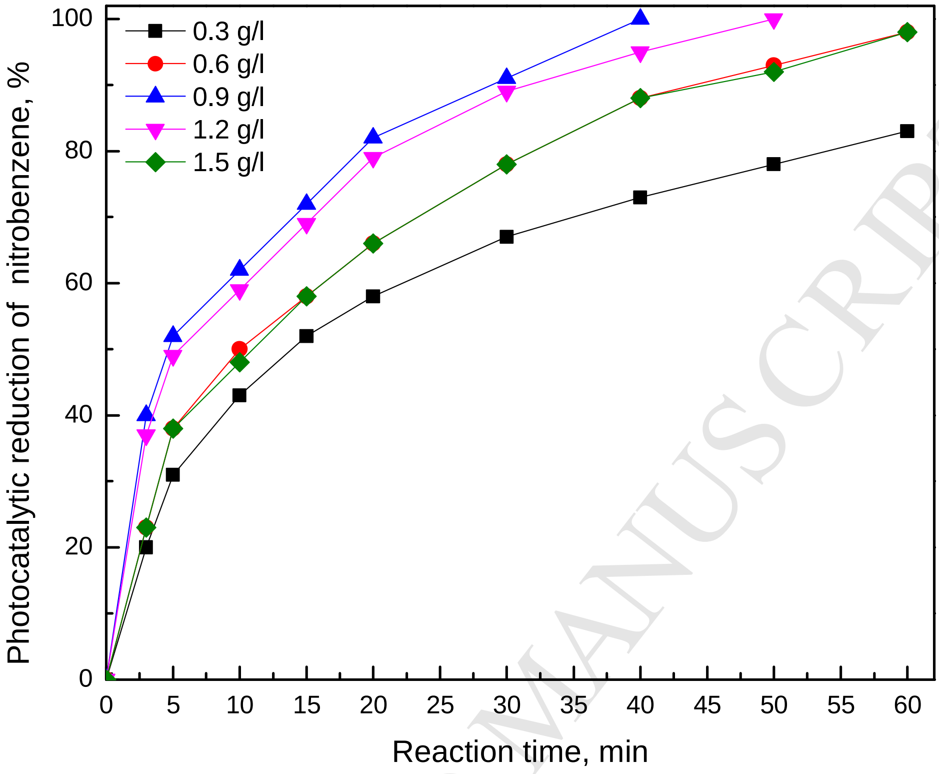
Photocatalytic reduction of nitrobenzene, %
Reaction time, min
0.3 g/l
0.6 g/l
0.9 g/l
1.2 g/l
1.5 g/l
0
20
40
60
80
100
0
5
10
15
20
25
30
35
40
45
50
55
60

Fig.10.

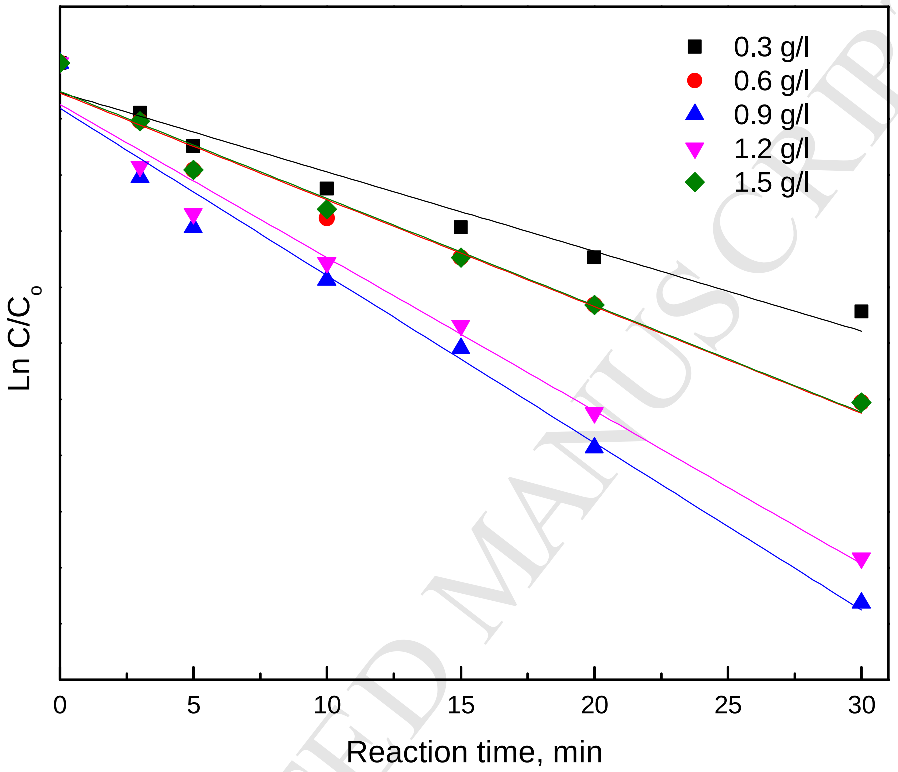
Ln C/C$_o$
Reaction time, min
0
5
10
15
20
25
30
0.3 g/l
0.6 g/l
0.9 g/l
1.2 g/l
1.5 g/l

Fig.11.

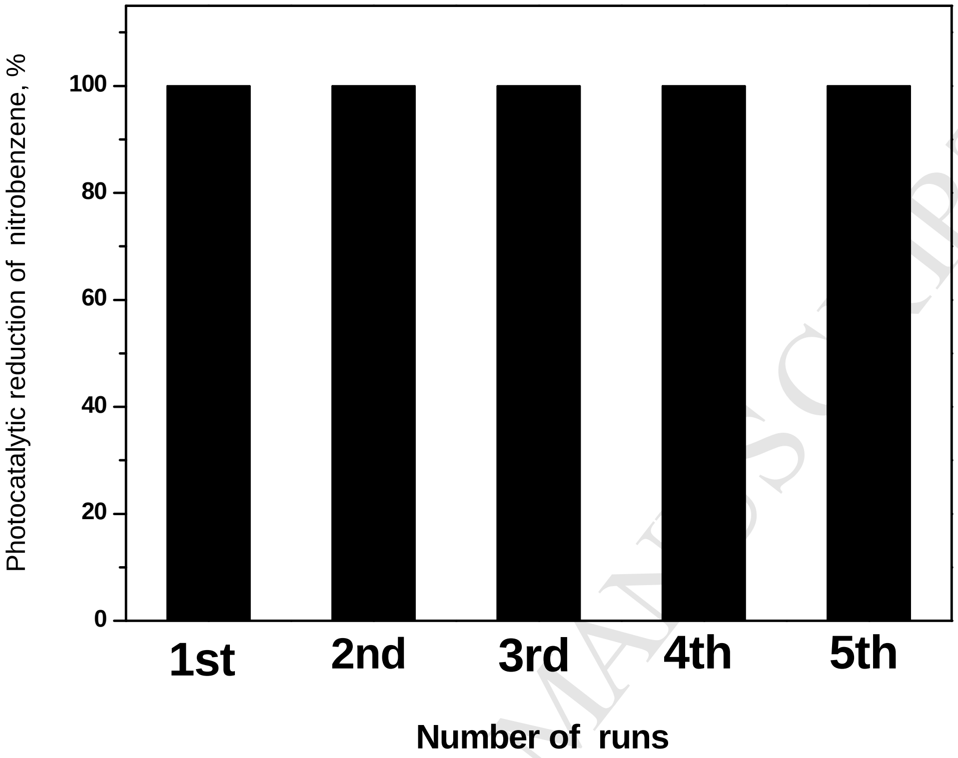
Photocatalytic reduction of nitrobenzene, %
0
20
40
60
80
100
1st
2nd
3rd
4th
5th
Number of runs

Fig.12.

Research Highlights

► **Pt-doped Nd_2O_3 hollow sphere was prepared by a template method**

► **Photocatalytic preparation of aniline under visible light was dependent on wt % of Pt .**

► **Catalyst re-use revealed the present photocatalyst remain effective and active after five cycles**